First-principles study of high-field-related electronic behavior of group-III nitrides

Qimin Yan, Emmanouil Kioupakis, Debdeep Jena, and Chris G. Van de Walle

First-principles study of high-field related electronic behavior of group-III nitrides

Qimin Yan,[1,2] Emmanouil Kioupakis,[1,3] Debdeep Jena,[4] and Chris G. Van de Walle[1]

[1]*Materials Department, University of California,*

Santa Barbara, California 93106-5050, USA

[2]*Molecular Foundry, Lawrence Berkeley National*

Laboratory, Berkeley, California 94720, USA

[3]*Department of Materials Science and Engineering,*

University of Michigan, Ann Arbor, Michigan 48109, USA and

[4]*Department of Electrical Engineering,*

University of Notre Dame, Notre Dame, Indiana 46556, USA

(Dated: August 26, 2014)

Abstract

Based on accurate band structures of AlN, GaN, and InN we report physical quantities related to high-field electron transport, including effective masses, energies of inflection points, and satellite valleys in the conduction band. The band structures are obtained from density functional theory with a hybrid functional, as well as many-body perturbation theory based on the G_0W_0 approach. We also calculate the electron-energy relaxation time due to the electron-LO-phonon interaction within the Fröhlich model. Our results provide insights into the physical origin of negative differential resistance and the high-frequency characteristics of group-III nitrides and their alloys under high-field operation.

PACS numbers: 71.20.Nr, 72.20.Jv, 85.60.Bt, 85.30.Fg

Nitride wide-band-gap semiconductors have important applications as high-power and high-temperature electronic devides. Particular interest has been focused on GaN and its use in heterojunction field-effect transistors as a powerful amplifier of microwave power.[1,2] The high-field performance of GaN-based electronic devices is related to two properties of the conduction band (CB): the nonparabolicity of the main CB valley characterized by an inflection point, and the existence of satellite valleys. Both of these can give rise to a negative differential resistance (NDR), where the drift velocity initially increases with the applied electric field to reach a maximum and then decreases with further increase in the field.

Inter-valley electron transfer to satellite valleys with heavier effective masses can generate an electron-transfer NDR, the so-called Gunn effect.[3,4] The upper frequency of radiation produced by the Gunn effect for traditional semiconductors such as GaAs and InP is on the order of 100 GHz,[5–7] determined by the inter-valley scattering which is relatively weak. On the other hand, under high field electrons can be excited above the inflection point and their semiclassical effective masses become negative. Attaining the maximum group velocity at the inflection point, electrons start to slow down under an applied field and can induce NDR even in the absence of any scattering mechanism.[8] The frequency of radiation associated with the negative-mass region close to the inflection point is determined by intra-band scattering and the strength of the electron-phonon interaction, and the characteristic frequency of radiation by this negative-mass effect can be on the order of THz.[9,10]

The relative ordering of the inflection point and the energy minima of the satellite valleys determines which mechanism dominates the velocity-field characteristics. Accurate band structures are thus crucial to address this issue. The empirical pseudopotential method (EPM) has been widely used to calculate nitride bands structures,[11,12] and several reports on high-field transport of electrons in GaN and AlN have been published.[11,13–16] Most EPM band-structure calculations identify the lowest satellite CB valley for GaN to be at the U point, along the L-M direction, but its precise position and energy vary widely among the different reports. In addition, EPM calculations usually produce an incorrect electron effective mass. In the present work, we obtain full band structures of nitride materials (including AlN, GaN, and InN) from advanced first-principles techniques including the hybrid functional approach and the G_0W_0 quasi-particle method based on the many-body perturbation theory. These band structures provide accurate information about the positions of inflection

points and satellite valleys.

The characteristic radiation frequency in the negative-mass region close to the inflection point is determined by intra-band scattering; therefore a quantitative determination of the electron scattering rate is also important. Electron relaxation times have also previously been calculated based on empirical models.[17] It has already been established that longitudinal optical (LO) phonon scattering dominates the electron mobility for AlGaN/GaN at and above room temperature.[18] In this work we will therefore focus on electron scattering due to the electron-LO-phonon interaction. Based on our accurate full band structure and using the Fröhlich model to describe the coupling between electrons and LO phonons, we quantitatively investigate the electron energy relaxation time due to electron-LO-phonon interactions in GaN.

Accurate knowledge of band structures and relaxation processes is also a crucial prerequisite for understanding the performance of optoelectronic devices. For instance, Auger recombination is being investigated as a cause of efficiency droop in nitride light emitting diodes (LED) both theoretically[19] and experimentally.[20] Iveland et $al.$[21] used electron emission spectroscopy to observe the generation of Auger electrons in a nitride LED under electrical-injection conditions, an observation that relies on high-energy electrons traveling through the p-type layer to the surface.

Our first-principles calculations are based on density functional theory using plane-wave projector augmented waves, as implemented in the VASP code.[22] We used the screened hybrid functional of Heyd, Scuseria, and Ernzerhof (HSE)[23] with the screening parameter set to a value of 0.2 Å^{-1}. The mixing parameter is adjusted to reproduce the experimental band gaps (0.34 for AlN, 0.29 for GaN, and 0.25 for InN). We use a plane-wave energy cutoff of 500 eV and a 6×6×4 Γ-centered k-point mesh. We verified that inclusion of spin-orbit coupling does not affect our results; this is because the conduction band is comprised almost exclusively of s states. The GW energies were calculated with exact-exchange-based G_0W_0 calculations[24] and interpolated throughout the Brillouin zone using the maximally localized Wannier function method[25] as in Ref. 26.

The band structure of the lowest CB of GaN, obtained from LDA, HSE, and G_0W_0 calculations, is shown in Fig. 1. The HSE band dispersion agrees very well with G_0W_0; indeed, the results are almost indistinguishable. Moreover, the effective masses obtained with HSE, namely $m_{\parallel}{=}0.20m_0$ (along the c-axis) and $m_{\perp}{=}0.19m_0$ (perpendicular to the c-axis) are

very close to those obtained with G_0W_0 ($m_\parallel$=0.19m_0, $m_\perp$=0.21m_0). G_0W_0 is currently the method of choice for band-structure calculations, and the close agreement indicates that HSE is a reliable band-structure method for group-III nitrides. On the other hand, the LDA band structure shows noticeable discrepancies in the band dispersion, also reflected by the considerable differences in effective masses ($m_\parallel$=0.16m_0, $m_\perp$=0.17m_0) compared with HSE and G_0W_0. We have also performed band-structure calculations with the generalized gradient approximation functional of Perdew, Becke, and Ernzerhof[?] (GGA-PBE) (not shown in Fig. 1); conduction-band dispersions obtained by LDA and GGA-PBE are essentially indistinguishable in the energy range from the conduction-band minimum (CBM) to the inflection points, and very similar to each other (and different from the HSE and G_0W_0 results) at higher energies.

The CBs of the three nitrides are shown in Fig. 2. Inflection points are present for all three nitrides, while three satellite valleys are located at Γ, K, and U points in the CBs; the energies are shown in Table I. The CBM at Γ is set as the energy zero. In AlN, three inflections points occur in the CB, along the Γ-A, Γ-K, and Γ-M directions. Only two inflection points are observed for GaN and InN, along the Γ-A and Γ-K directions. Table I also shows that the energy of the inflection points in GaN is considerably different between HSE and LDA calculations, HSE being $\sim$0.2 eV higher in energy, again indicating that the accuracy of LDA is insufficient.

Three satellite valleys are observed, at the U (between L and M), K, and A points. Interestingly, the next-higher CB minima are located at different points in the Brillouin zone for the three materials. The secondary minimum in GaN is the U valley, while in InN it is the A valley. For AlN the minima at U and K are very close, and both these minima are quite close in energy to the CBM at Γ.

In Fig. 3 we plot the energies of inflection points along Γ-A and Γ-M directions and satellite U and A valleys in AlGaN and InGaN alloys assuming that these quantities can be linearly interpolated between their binary parent compounds. The inflection points in GaN are 0.8 to 1.0 eV below the bottom of the U valley, while in AlN the inflection points are 0.5 to 0.9 eV above the U valley. From the linear interpolation, we infer that the critical point where the inflection point and the bottom of the U valley are at the same energy is located at $\sim$64% Al composition. This indicates that negative-mass NDR can be present in AlGaN alloys with Al content below 64%, while in alloys with higher Al content intervalley

electron-transfer NDR would dominate.

The inflection point in InN is at 0.89 eV above the CBM while the secondary valleys are at much higher energies. It therefore might seem that InN is a good candidate for negative-mass NDR. However, it is necessary to also compare the energies of inflection points to the size of the band gap. If the electron kinetic energy exceeds the band gap, impact ionization becomes possible, since electrons can lose their energy by exciting electron-hole pairs. Therefore, NDR may not be possible in InN. To quantitatively address this issue, we plot the band gaps of the three nitrides (HSE values 6.13 eV for AlN, 3.50 eV for GaN, and 0.67 eV for InN) and interpolated values for their alloys in Fig. 3. We used bowing parameters of 1.0 eV for AlGaN[28] and 1.36 eV for InGaN,[29] the latter being a "global" value providing the best quadratic fit over the entire alloy range; as noted in Ref.29, bowing is much stronger at low In content. Figure 3 shows that the critical point where the energy of the inflection point above the CBM is equal to the alloy band gap occurs at 87% In composition. In InGaN alloys with higher In content negative-mass NDR could be suppressed by impact ionization. We note that nonlinear effects were not considered when interpolating the energy positions of valleys and inflection points. Since such effects would result from a *difference* in bowing between two energy positions in the CB, their inclusion is unlikely to affect any of our conclusions.

The characteristic frequency for negative-mass NDR related to inflection points is determined by intra-band scattering, with a scattering rate depending on the strength of the electron-phonon interaction. The energy relaxation time (as opposed to the momentum relaxation time) is the relevant quantity. We focus on the coupling between electrons and LO phonons described by the Fröhlich model.[30] This assumes the interactions involve phonons with small crystal momenta,[19] an assumption that is valid in the case of high-field operation because high-energy electrons can be scattered effectively by intra-band transitions with a small change in momentum.

According to Fermi's golden rule, the electron energy relaxation time τ_k due to scattering from an initial state to a final state by electron-phonon interaction is given by

$$\frac{1}{\tau_{\boldsymbol{k}}} = \frac{2\pi}{\hbar} \sum_{\boldsymbol{q}} \frac{\hbar\omega_{\boldsymbol{q}}}{\epsilon_{\boldsymbol{k}}} |g(\boldsymbol{q})|^2 \tag{1}$$

$$\left[(n_{\boldsymbol{q}} + 1)\, \delta(\epsilon_{\boldsymbol{k}} - \epsilon_{\boldsymbol{k}+\boldsymbol{q}} - \hbar\omega_{\boldsymbol{q}}) - n_{\boldsymbol{q}}\delta(\epsilon_{\boldsymbol{k}} - \epsilon_{\boldsymbol{k}+\boldsymbol{q}} + \hbar\omega_{\boldsymbol{q}}) \right].$$

ϵ denotes the band energy of an electron and k represents the wave vector of an initial state. $\hbar\omega_q$ is the LO phonon energy corresponding to the wave vector q mapped to the

first Brillouin zone. Since the dispersion of LO phonons is low, and their frequencies do not vary much along different directions, we take the LO phonon energy in GaN to be constant (equal to 92 meV)[31] in our calculations. $n_q = 1/(e^{\hbar\omega_q/kT} - 1)$ is the occupation number of phonons. The first term in Eq. (1) corresponds to phonon-emission and the second to phonon-absorption processes. The scattering rate is determined by two aspects: how many final states are available close to a specific electron energy and how strong the coupling is between the initial state and all possible final states. To achieve the required accuracy, energies of electronic states on a dense grid in the reciprocal lattice obtained by LDA calculations are interpolated from those on a coarse grid by using maximally localized Wannier functions.[25]

The interaction Hamiltonian is described by the Fröhlich model:

$$g_{\text{Fröhlich}}(q) = \frac{q}{q^2 + q_{\text{TF}}^2} \sqrt{\frac{2\pi\hbar\omega_{\text{LO}}}{V_{\text{cell}}} \left(\frac{1}{\varepsilon_\infty} - \frac{1}{\varepsilon_0} \right)}.$$

The static dielectric constant ε_0 and high frequency dielectric constant ε_∞ used in our calculations for GaN are 10.4 and 5.35, respectively.[32,33] The screening of the Coulomb interaction due to the free carriers is taken into account by introducing the screening wave vector q_{TF} given by the Thomas-Fermi theory for degenerate carrier concentrations ($n > 10^{18}$ cm^{-3} for GaN at $T = 300$ K, where n is the free-electron density) and the Debye theory for non-degenerate carrier concentrations To obtain converged results, we used a gaussian broadening of 50 meV for the delta function and interpolated the energies of electronic states from a 8×8×8 coarse grid in reciprocal space to a dense grid of 192×192×96 using the maximally localized Wannier function method.[25]

Figure 4 shows the calculated electron energy relaxation time for electrons in the lowest conduction band of GaN along the Γ-A and Γ-M directions. Results are shown for 300 K; calculations at 200 K and 400 K reveal that, for the energies of interest, the relaxation times change by less than a factor of two over this temperature range. If the energy of the initial electronic state is below 92 meV, the maximum energy released is smaller than the LO-phonon energy, and LO-phonon emission is thus prohibited. Scattering can then only occur by *absorbing* an LO phonon, which would lead to a negative energy relaxation time according to Eq. (1); these negative values are not shown in the figure. In reality, acoustic phonons would allow phonon emission at energies below 92 meV. As justified above, LO-phonon scattering is known to be dominant in the energy range of interest for high-field

transport, which is well above 92 meV.

Along both the Γ-A and Γ-M directions, at low to medium carrier density ($<$ 1×10^{19}cm^{-3}), the energy relaxation time increases with increasing electron energy in the energy range between 0.25 and 2 eV. At higher carrier density, the energy relaxation time decreases with increasing electron energy. Close to the inflection points, the energy relaxation time is in the range 10^{-13} to 10^{-12} s, the values being very sensitive to the carrier density in the sample. For example, for an electron close to the inflection point with a wave vector along the Γ-A direction, the relaxation time increases by about one order of magnitude if the carrier density increases from 1×10^{16}cm^{-3} to 1×10^{19}cm^{-3}, due to significant screening of the electron-LO-phonon interaction. Also included in Fig. 4(a) is a comparison with previous results based on the empirical pseudopotential method[17] for a carrier density of 10^{17} cm^{-3}, which included scattering contributions from all phonons. The good agreement with our first-principles calculations, which include only optical phonon scattering, indicates that the contribution of acoustic phonons to the final scattering rate is indeed not significant.

Nonparabolicity in the CB can significantly affect the relaxation time. To analyze this effect, we compared our calculated relaxation time along Γ-A in the absence of carrier screening with the analytical solution[34] that assumes a parabolic band dispersion, using our calculated effective mass. At energies close to the CBM, the calculated scattering rates agree well with the analytical solutions. However, once the electron energy exceeds 0.3 eV, the deviation of the numerical results from the analytical solution becomes large. For instance, the numerical data are smaller than the analytical results by around a factor of two at k-points close to the Brillouin-zone boundary along the Γ-A direction.

In summary, we reported accurate band structures for AlN, GaN, and InN based on first-principles calculations, and extracted parameters relevant for high-field transport, including the energies of inflection points and the minima of satellite valleys. Based on this detailed information, we predict that negative-mass NDR can be realized in GaN, while in AlN electron-transfer NDR will be dominant. Based on a linear interpolation of these quantities we estimate a critical Al composition (64%) for AlGaN alloys, above which the negative-mass NDR becomes dominant. For InN, the negative-mass NDR will be hindered by impact ionization; the critical In composition for InGaN alloys below which negative-mass NDR becomes possible was estimated to be 87%. We also calculated the energy relaxation time due to the electron-LO-phonon interaction described by the Fröhlich model. A striking

7

difference between GaN (and InN) and other III-V compounds such as GaAs or InAs is the very large intervalley separation, which is large enough to provide access to negative-mass energy states. At the same time, the large CB offsets provide the band alignments necessary to inject carriers into these negative-effective mass energy windows in heterostructures by hot-electron injection. Our results and analysis provide a theoretical platform to investigate such high-field phenomena in nitride devices.

[1] T. Palacios, A. Chakraborty, S. Heikman, S. Keller, S. P. DenBaars, and U. K. Mishra, IEEE Electron Device Lett. **27**, 13 (2006).

[2] M. Higashiwaki, T. Matsui, and T. Mimura, IEEE Electron Device Lett. **27**, 16 (2006).

[3] J. B. Gunn, Solid State Commun. **1**, 88 (1963).

[4] H. Kroemer, Proc. IEEE **52**, 1736 (1964).

[5] S. J. J. Teng and R. E. Goldwasser, IEEE Electron Device Lett. **10**, 412 (1989).

[6] A. Khalid, N. J. Pilgrim, G. M. Dunn, M. C. Holland, C. R. Stanley, I. G. Thayne, and D. R. S. Cumming, IEEE Electron Device Lett. **28**, 849 (2007).

[7] H. Eisele and R. Kamoua, IEEE Trans. Microw. Theory Tech. **52**, 2371 (2004).

[8] B. K. Ridley, W. J. Schaff, and L. F. Eastman, J. Appl. Phys. **97**, 094503 (2005).

[9] H. Krömer, Phys. Rev. **109**, 1856 (1958).

[10] Z. S. Gribnikov, R. R. Bashirov, and V. V. Mitin, IEEE J. Sel. Top. Quant. Electron. **7**, 630 (2001).

[11] C. Bulutay, B. K. Ridley, and N. A. Zakhleniuk, Phys. Rev. B **62**, 15754 (2000).

[12] D. Fritsch, H. Schmidt, and M. Grundmann, Phys. Rev. B **69**, 165204 (2004).

[13] S. Krishnamurthy, M. van Schilfgaarde, A. Sher, and A.-B. Chen, Appl. Phys. Lett. **71**, 1999 (1997).

[14] C. Bulutay, B. K. Ridley, and N. A. Zakhleniuk, Phys. Rev. B **68**, 115205 (2003).

[15] A. Dyson and B. K. Ridley, J. Appl. Phys. **104**, 113709 (2008).

[16] V. M. Polyakov and F. Schwierz, J. Appl. Phys. **99**, 113705 (2006).

[17] E. Bellotti and F. Bertazzi, *Transport Parameters for Electrons and Holes* (Wiley-VCH Verlag GmbH Co. KGaA, 2007), pp. 69–93.

[18] L. Hsu and W. Walukiewicz, Phys. Rev. B **56**, 1520 (1997).

[19] E. Kioupakis, P. Rinke, K. T. Delaney, and C. G. Van de Walle, Appl. Phys. Lett. **98**, 161107 (2011).

[20] Y. C. Shen, G. O. Mueller, S. Watanabe, N. F. Gardner, A. Munkholm, and M. R. Krames, Appl. Phys. Lett. **91**, 141101 (2007).

[21] J. Iveland, L. Martinelli, J. Peretti, J. S. Speck, and C. Weisbuch, Phys. Rev. Lett. **110**, 177406 (2013).

[22] G. Kresse and J. Furthmuller, Phys. Rev. B **54**, 11169 (1996).

[23] J. Heyd, G. E. Scuseria, and M. Ernzerhof, J. Chem. Phys. **124**, 219906 (2006).

[24] P. Rinke, M. Winkelnkemper, A. Qteish, D. Bimberg, J. Neugebauer, and M. Scheffler, Phys. Rev. B **77**, 075202 (2008).

[25] N. Marzari, A. A. Mostofi, J. R. Yates, I. Souza, and D. Vanderbilt, Rev. Mod. Phys. **84**, 1419 (2012).

[26] E. Kioupakis, P. Rinke, A. Schleife, F. Bechstedt, and C. G. Van de Walle, Phys. Rev. B **81**, 241201 (2010).

[27] J. P. Perdew, K. Burke, and M. Ernzerhof, Phys. Rev. Lett. **77**, 3865 (1996).

[28] F. Yun, M. A. Reshchikov, L. He, T. King, H. Morkoc, S. W. Novak, and L. Wei, J. Appl. Phys. **92**, 4837 (2002).

[29] P. Moses, M. S. Miao, Q. Yan, and C. G. Van de Walle, J. Chem. Phys. **134**, 084703 (2011).

[30] P. Yu and M. Cardona, *Fundamentals of Semiconductors: Physics and Materials Properties* (Springer, 2010).

[31] M. Giehler, M. Ramsteiner, O. Brandt, H. Yang, and K. H. Ploog, Appl. Phys. Lett. **67**, 733 (1995).

[32] A. Barker Jr and M. Ilegems, Phys. Rev. B **7**, 743 (1973).

[33] D. D. Manchon, A. S. Barker, P. J. Dean, and R. B. Zetterstrom, Solid State Commun. **8**, 1227 (1970).

[34] B. K. Ridley, *Quantum Processes in Semiconductors* (Oxford University Press, USA, 2000).

TABLE I: Energies (in eV) of inflection points in the conduction band along different directions in the reciprocal lattice, and of the minima of satellite valleys for AlN, GaN, and InN. The CBM is set as the energy zero.

	method	Γ-A	Γ-M	Γ-K	U valley	K valley	A valley
AlN	HSE	1.19	1.08	1.51	0.61	0.62	2.41
GaN	HSE	1.13	1.27	-	2.13	3.03	2.49
	LDA	0.90	1.00	-	2.34	4.33	2.28
InN	HSE	0.89	1.01	-	3.51	5.20	2.73
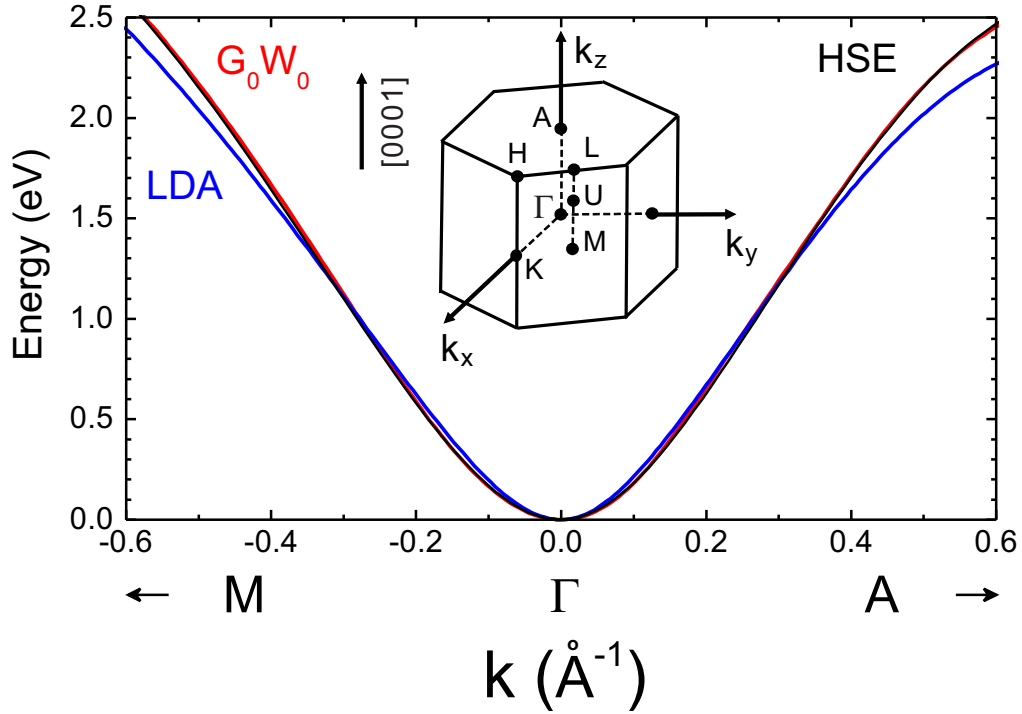
FIG. 1: Lowest conduction band of GaN obtained from LDA, HSE, and G_0W_0 methods. Note that the HSE and GW results are almost indistinguishable. The inset shows the Brillouin zone, with the high-symmetry points labeled.
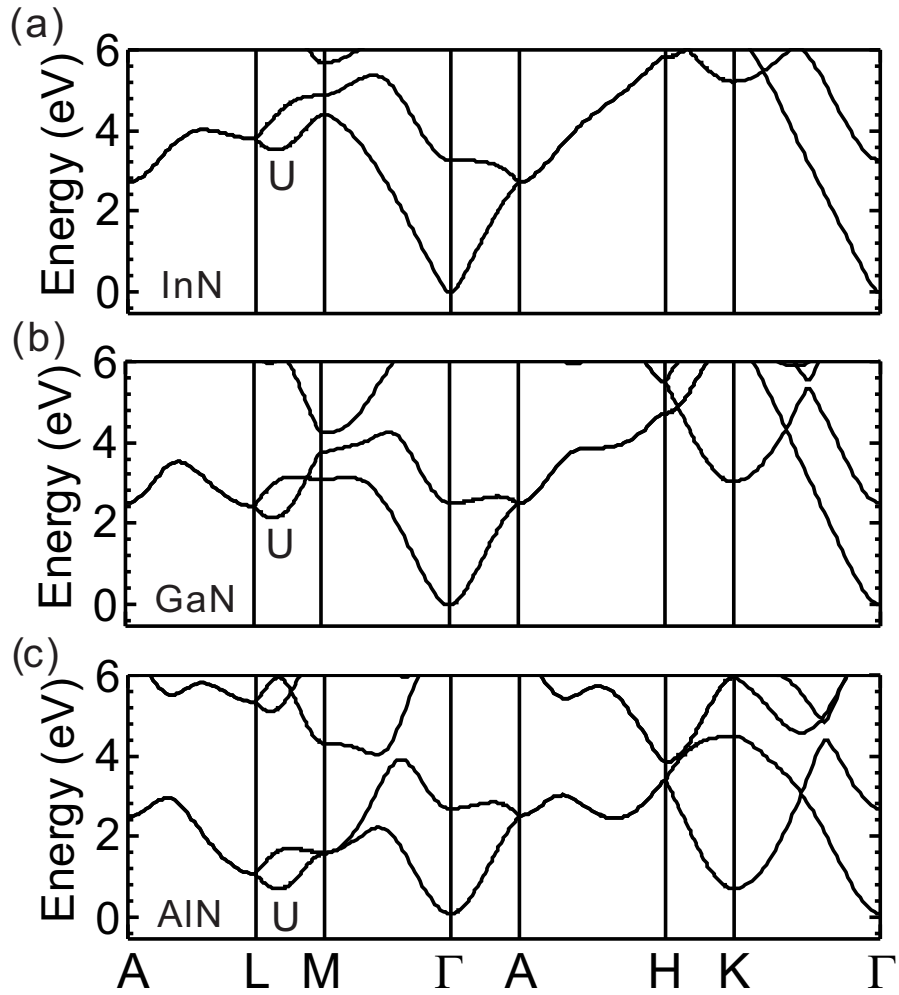
FIG. 2: Conduction-band structures of (a) InN, (b) GaN, and (c) AlN obtained from the HSE method. The energy zeros are set at the conduction-band minima.
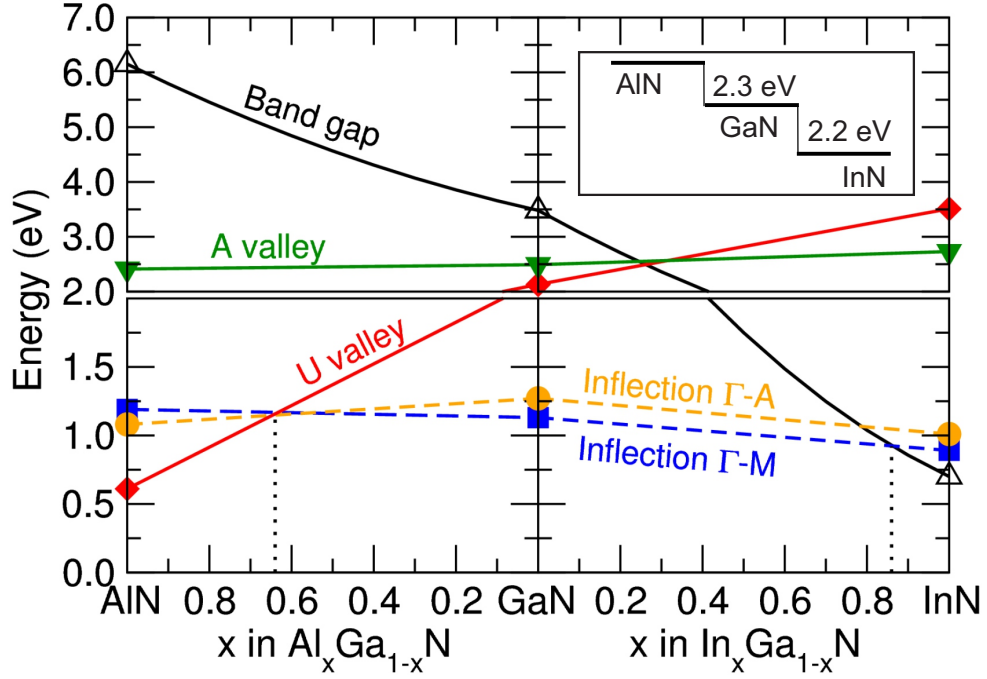
FIG. 3: Band-structure related quantities for AlN, GaN, and InN, as well as AlGaN and InGaN alloys: experimental band gaps, and energies of inflection points and of U and A valleys, referenced to the CBM. Note the change in scale between lower and upper panels. The vertical dashed lines denote crossing points between physical quantities relevant for NDR. The inset shows the CB offsets between the CBM (at Γ) in AlN, GaN and InN (from Ref. 29).
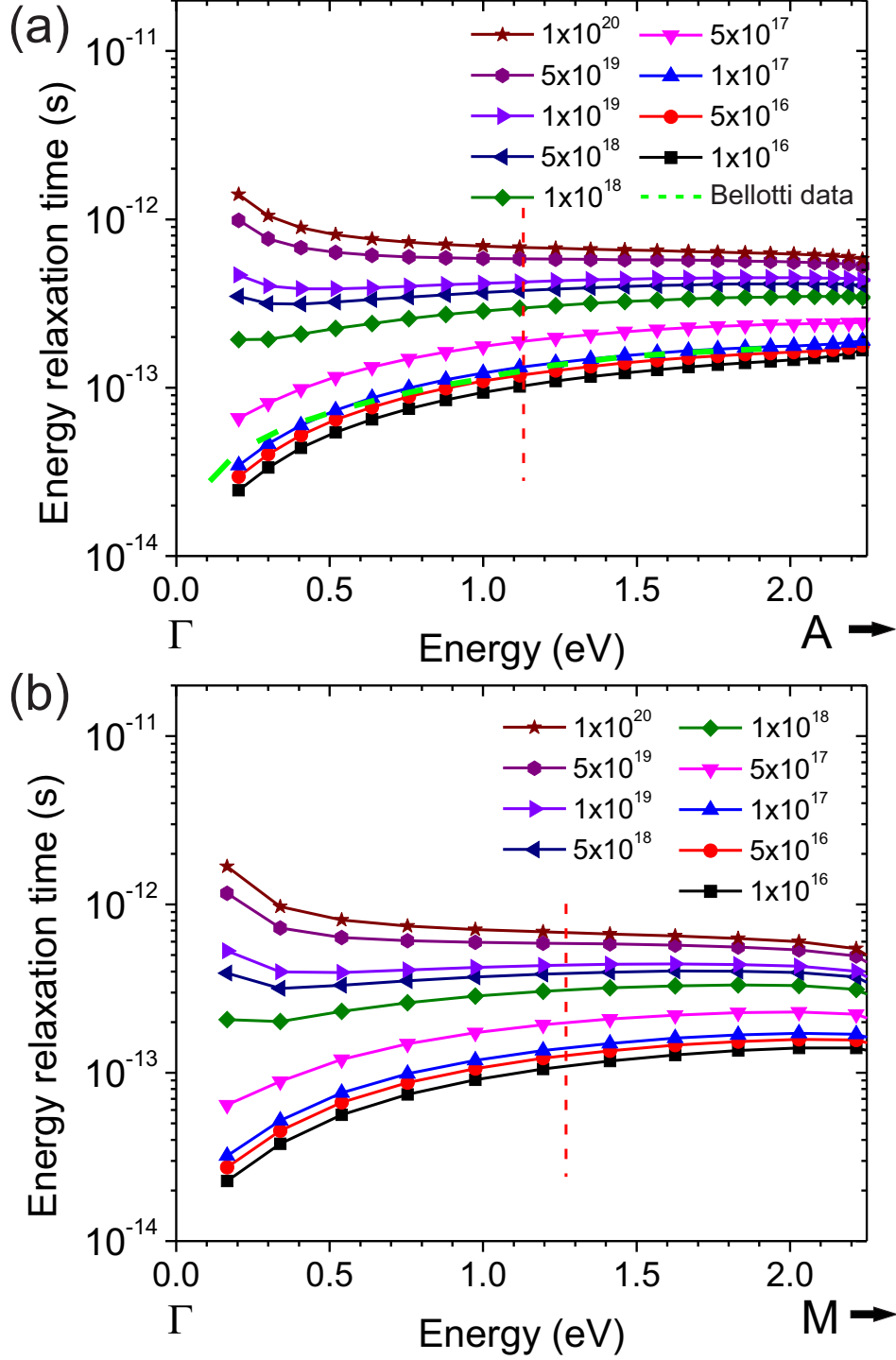
FIG. 4: Calculated energy relaxation time due to electron-LO-phonon interaction for electrons in the CB of GaN along (a) Γ-A and (b) Γ-M directions. The curves are given for various carrier concentrations (in cm^{-3}). The vertical dashed lines denote the energies of inflection points. The Bellotti data are from Ref. 17.

15